

Supplementary Information

Morphological analysis of cerium oxide stabilized nanoporous gold catalysts by soft X-ray ASAXS

C. Rumancev^a, A. R. von Gundlach^a, S. Baier^b, A. Wittstock^c, J. Shi^c, F. Benzi^b, T. Senkbeil^a, S. Stuhr^a, V. M. Garamus^d, J.-D. Grunwaldt^b, A. Rosenhahn^a

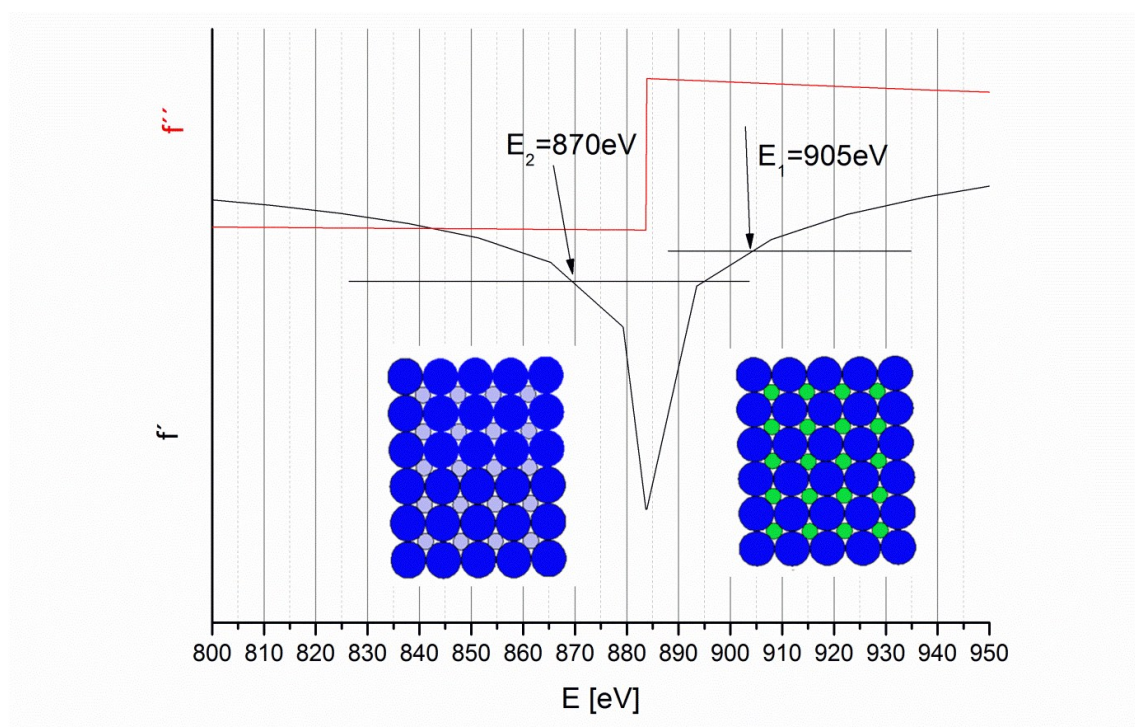
^aAnalytical Chemistry - Biointerfaces, Ruhr-University Bochum, Universitätsstr. 150, 44780 Bochum, Germany

^bInstitute for Chemical Technology and Polymer Chemistry, Karlsruher Institut für Technologie (KIT), Engesserstr. 20, 76131 Karlsruhe, Germany

^cInstitute of Applied and Physical Chemistry, University of Bremen, P.O. Box 330 440 28359 Bremen, Germany

^dHelmholtz-Zentrum Geesthacht, Zentrum für Material- und Küstenforschung GmbH, Max-Planck-Straße 1, 21502 Geesthacht, Germany

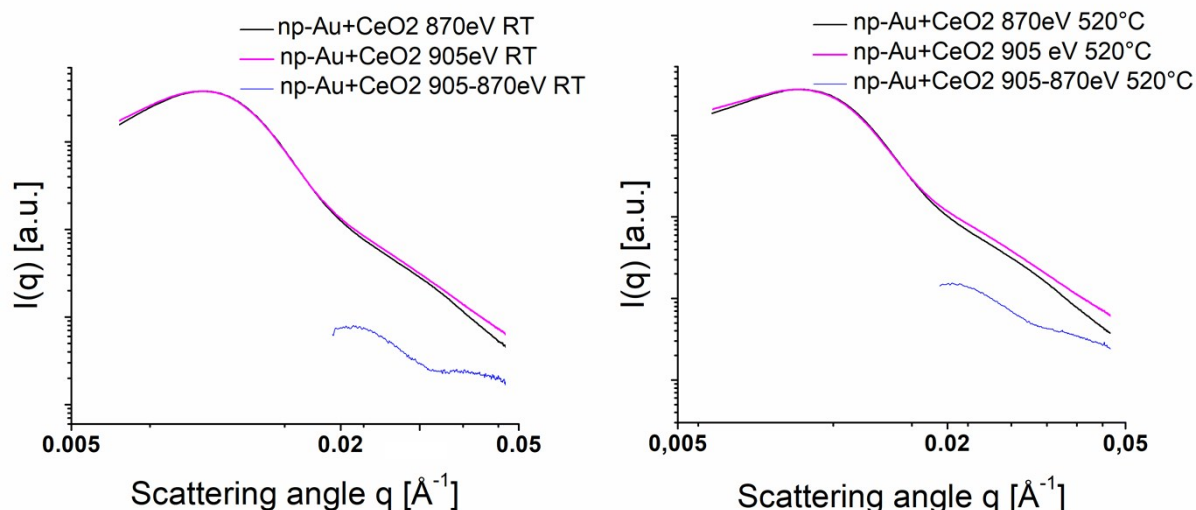
The contrast in the ASAXS experiments is based on the anomalous scattering contrast at the Ce M edge. Figure S1 shows the real (f') and imaginary (f'') dispersion coefficients of the anomalous scattering amplitude as function of the photon energy. The resonance in this energy range is the origin of the obtained ASAXS contrast and SAXS curves were measured at 870 eV and 905 eV which causes a change in both, f' and f'' .



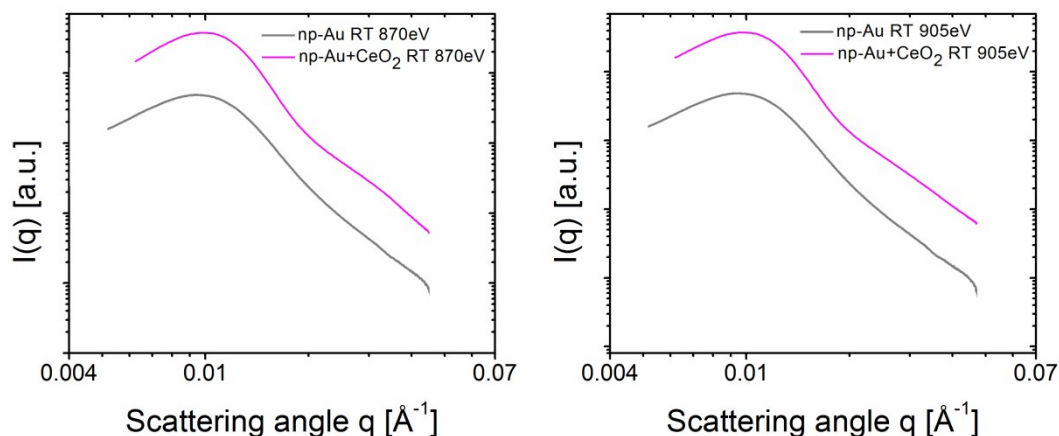
Supplementary Figure S1: Anomalous scattering amplitude as a function of photon energy^{50,51}. f' (black line) and f'' (red line) are real and imaginary dispersion coefficient⁵². The coefficient f' is proportional to the atomic scattering factor and f'' is proportional to the absorption coefficient. The change in f' as a function of energy is responsible for the ASAXS signal. Standard ASAXS experiments operate at two energies: one far below the edge (E_2) and one close to the edge (E_1). When compared to a surrounding matrix (here Au) that does not change with energy: at E_2 both elements are 'visible'

whereas close to the absorption edge, the atomic scattering factor of the element of interest decreases and it does not contribute to the overall scattering pattern. In our measurements the energies $E_1=905$ eV and $E_2=870$ eV were used. Since the atomic scattering factor f' is lower at E_2 the contribution of cerium can be obtained through the difference: $I(E_1) - I(E_2)$. Both cases are clarified with inserted images, blue spheres are the gold particles (here is no changes in intensity) and small grey and green spheres are ceria particles. The contribution to the overall scattering pattern changes with energy near the edge.

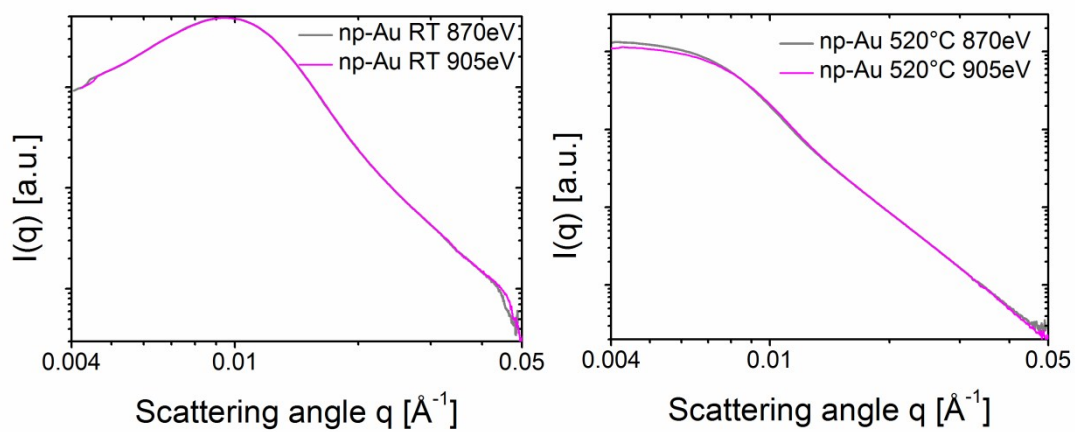
The ASAXS curves in Figure 3 were calculated by measuring the SAXS signal at two different photon energies (870 eV and 905 eV). Figures S2-S4 show the raw data used to calculate the scattering intensities for the ASAX plot in Figure 3.



Supplementary Figure S2: Calculation of the ceria ASAXS intensity. The SAXS intensities were normalized on the peak at 0.01 \AA^{-1} and subtracted $I(E_1)-I(E_2)$. The pure ceria contribution is shown in blue curve.



Supplementary Figure S3: Pure np-Au in comparison with $\text{CeO}_2/\text{np-Au}$. The Au main peak remains on the same position.



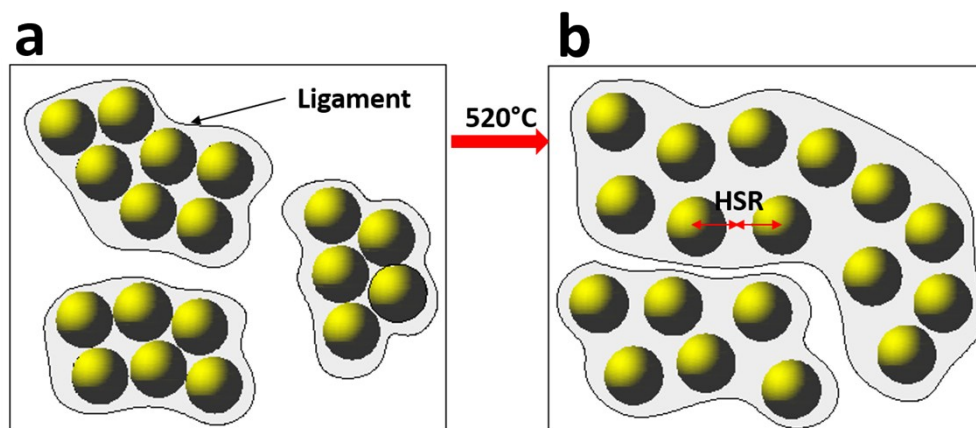
Supplementary Figure S4: Comparison between np-Au at different energies. SAXS intensities were normalized on the gold main peak at 0.01 \AA^{-1} .

Table S1 supplements Table 1 and shows in addition the D_{max} values, HSR and the obtained volume fractions.

Sample	D_{MAX} [Å]	Hard sphere radius (HSR) [Å]	Volume Fraction
np-Au RT	440	285 ±1,56	0.225 ±0,37
np-Au 520°C	790	410 ±1,30	0.08 ±0,34
np-Au/CeO ₂ RT	430	270 ±2,25	0.265 ±0,05
np-Au/CeO ₂ 520°C	450	270 ±2,25	0.225 ±0,37
CeO ₂ RT	220	141 ±0,89	0.3 ±0,48
CeO ₂ 520°C	210	141 ±0,89	0.17 ±0,25

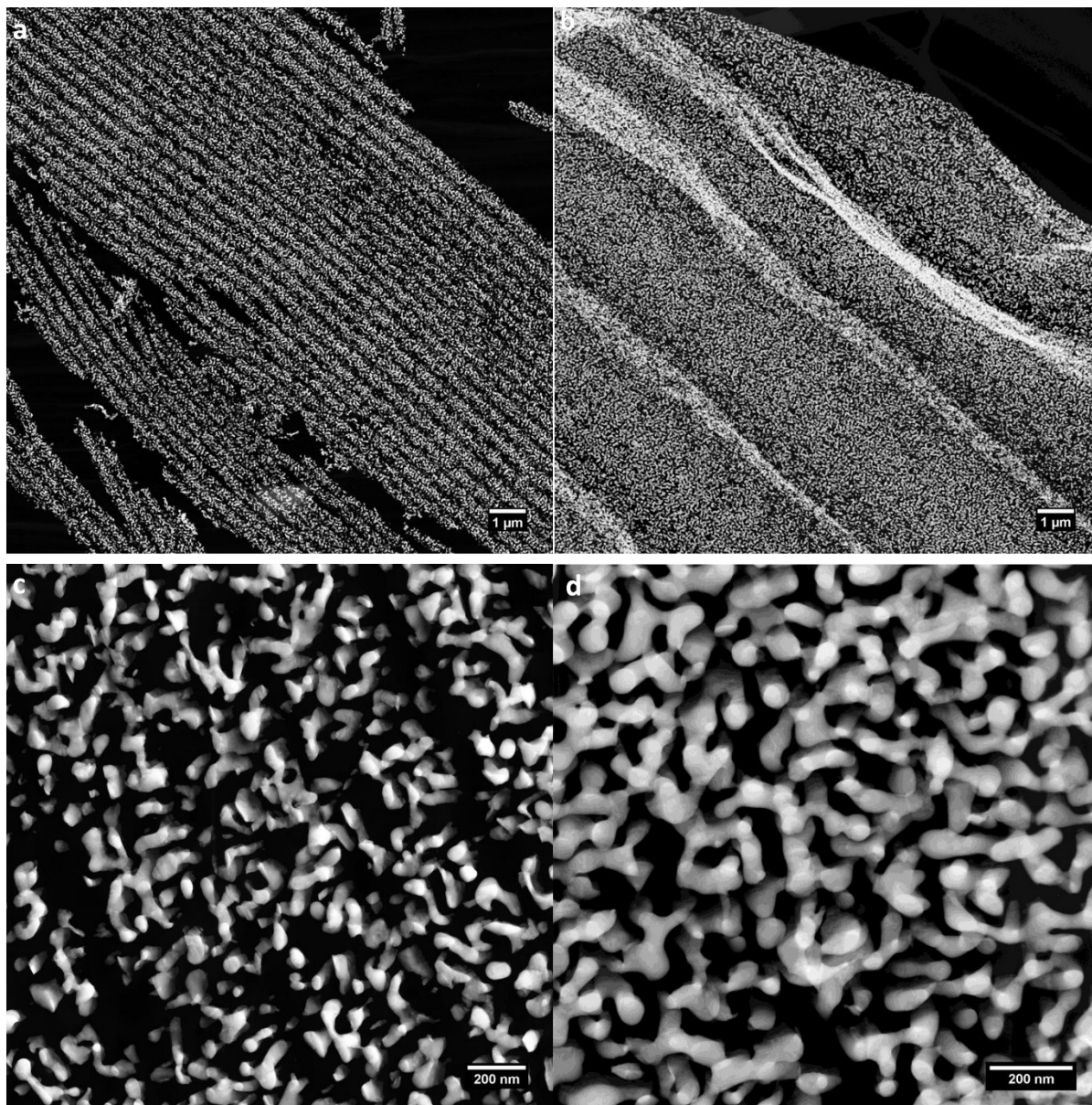
Supplementary Table S1: Iteratively optimized modeling parameters: it is necessary to select the maximal interparticle distance (D_{max}) region for an indirect Fourier transformation. The interaction between nanoparticles forming a ligament are modeled using a hard sphere interaction potential. The hard sphere radius (HSR) defines the radius around a particle at which the interaction occurs while the volume fraction (VF) defines the amplitude of the interaction.

Figure S5 shows a schematic model how the obtained values from the SAXS measurements could be connected to a coarsening of the structure of the gold ligaments.



Supplementary Figure S5: Ligaments (in grey) are composed of spherical building (yellow black) blocks with HSR between. Before annealing (a) and after (b). Without Ceria deposits annealing leads to coarsening and increase of HSR.

In a previous study it was found that annealing of the np-Au catalysts leads to a coarsening of the gold structure already at temperatures of 250°C (Baier et al., RSC Adv.,2016, 6, 83031, DOI: 10.1039/c6ra12853j). Some STEM-HAADF images showing the same trend are presented in Figure S6. The coarsening gets immediately obvious as the size of the gold ligaments increases.



Supplementary Figure S6: STEM-HAADF image of a np-Au sample before (a, c) and after annealing to 250°C (b, d).